



LAMB WAVE DECOMPOSITION USING COMCENTRIC RING AND CIRCULAR PIEZOELECTRIC TRANSDUCERS

Chulmin Yeum¹, Hoon Sohn¹, Jeong Beom Ihn²

¹ Department of Civil and Environment Engineering, Korea Advanced Institute of Science and Technology

² Boeing Research & Technology, Seattle, WA

Presented at EWSHM 2010, Sorrento, June 29, 2010

KAIST



This document contains confidential and proprietary information owned by
KAIST and Boeing. The distribution is limited.



1 Introduction

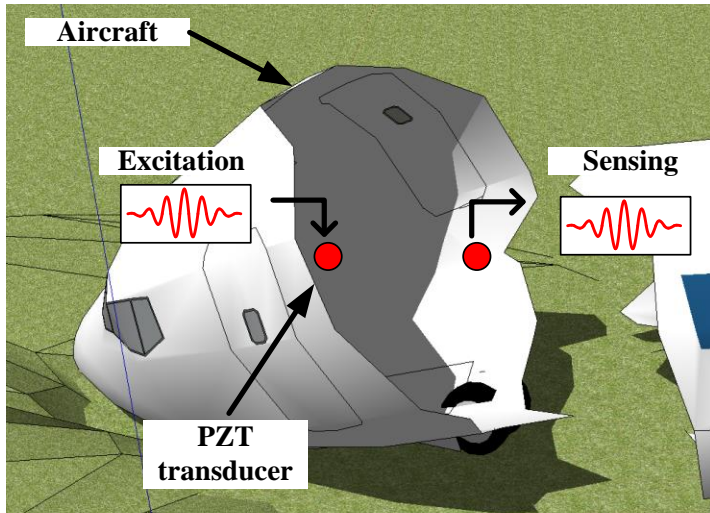
2 Theoretical Formulation

3 Numerical Simulation

4 Test Results

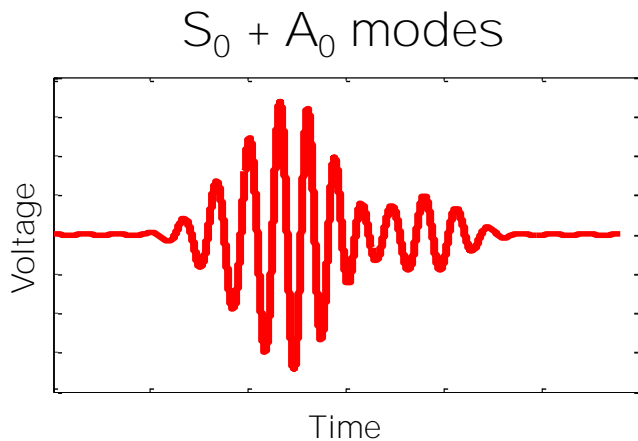
5 Conclusion

Motivation

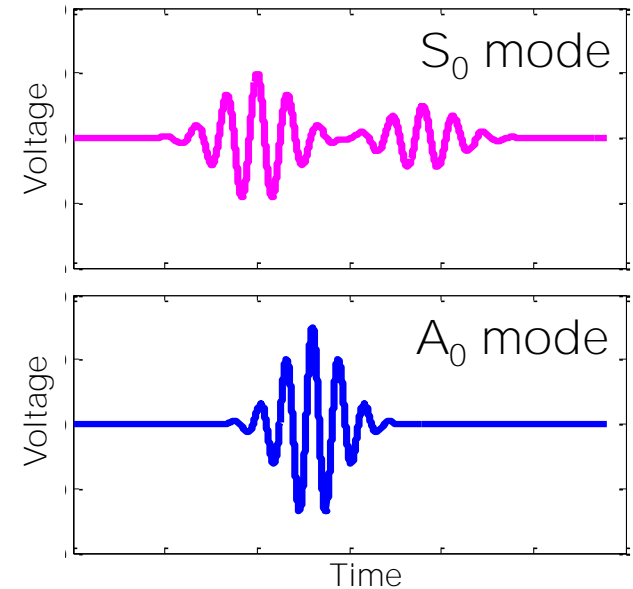


Surface-mountable piezoelectric transducer based SHM techniques have been widely used for monitoring of aircraft structures.

How can we **instantaneously** extract a **user-specified fundamental Lamb wave mode** from measured Lamb wave signals **using one sided attached PZT transducers**?



How (?)





- **Research objectives**

- Decomposition of fundamental Lamb wave (S_0 and A_0) modes** from measured signals without PZT size adjustment and frequency tuning

- **Advantages of the proposed technique**

- PZTs need to be placed only **a single surface** of the structure
 - Mode decomposition can be performed at any desired frequency **without physical adjustment of the PZT size and/or spacing**
 - Both S_0 and A_0 modes can be simultaneously decoupled and identified **at any driving frequency**
 - A circular design of the dual PZT allows **omni-directional** Lamb wave decomposition



- **Placement of collocated PZTs on both surfaces**

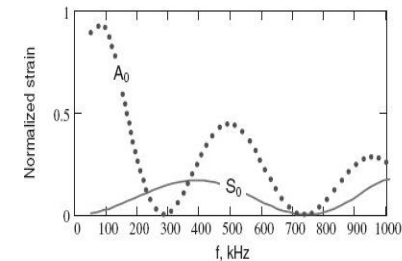
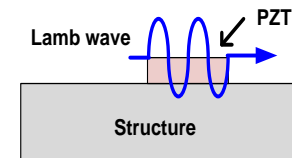
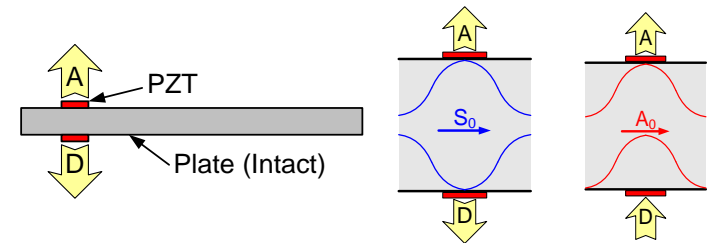
Using PZT poling directionality in Lamb wave propagation [Viktorov(1967),Kim (2007)]

Limitation: Accessibility to both surfaces of a structure and difficulty of precise placement of collocated PZTs

- **Tuning of driving frequency and/or the PZT size**

Selection of a specific frequency and/or the PZT size where the target mode is predominant [Giurgitiu (2005)]

Limitation: Possible only at a specific frequency and for a fixed PZT size





1 Introduction

2 Theoretical Formulation

3 Numerical Simulation

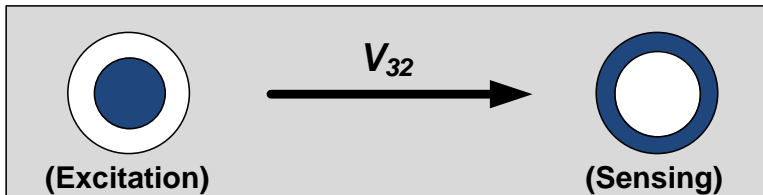
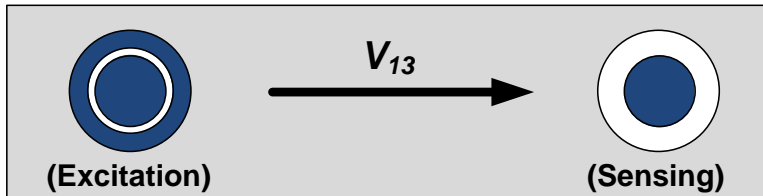
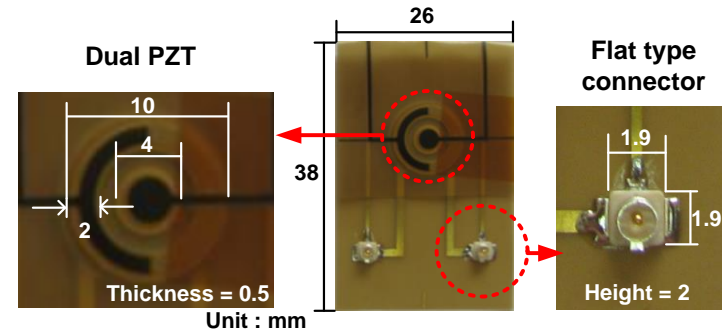
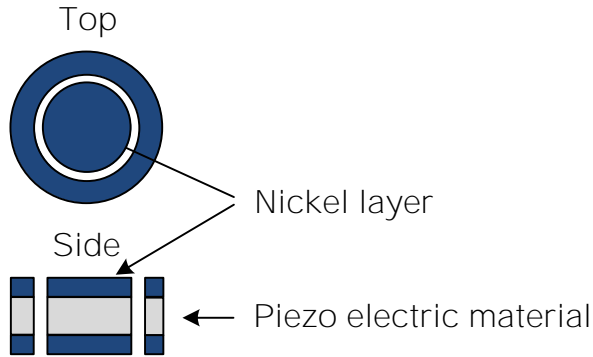
4 Test Results

5 Conclusion

Description of a Dual PZT and Signal Notation



Schematic drawing and picture of the dual PZT



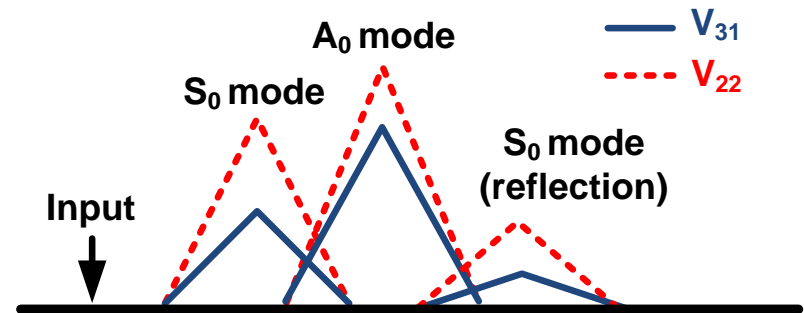
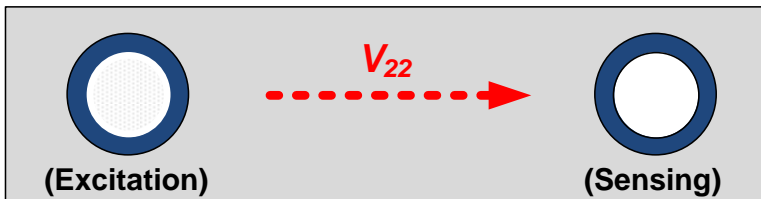
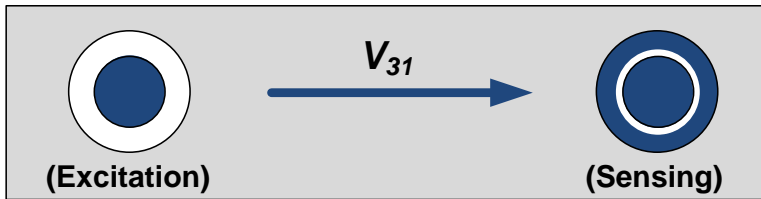
Signals obtained by dual PZTs

By activating different parts of the excitation and sensing dual PZTs, nine different response signals (V_{ij})

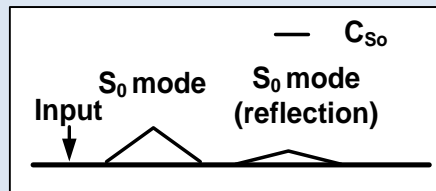
$$V_{ij}, i \text{ and } j = 1, 2 \text{ and } 3$$

The subscripts, 1, 2 and 3 denote the entire dual PZT, the other ring and the inner circular PZT, Respectively.

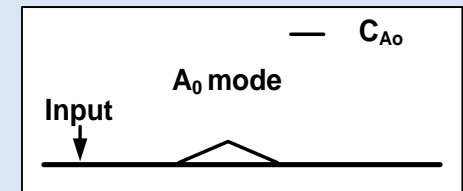
Overview of the Proposed Mode Decomposition Technique



$$V_{13} = S_{31} \times C_{S_0} + A_{31} \times C_{A_0} = S_{31} \times$$



$$+ A_{31} \times$$



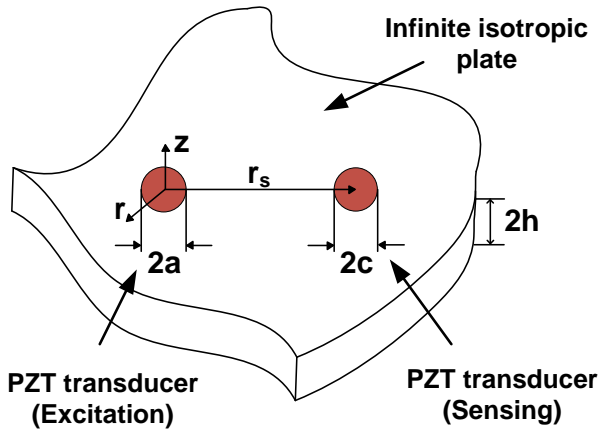
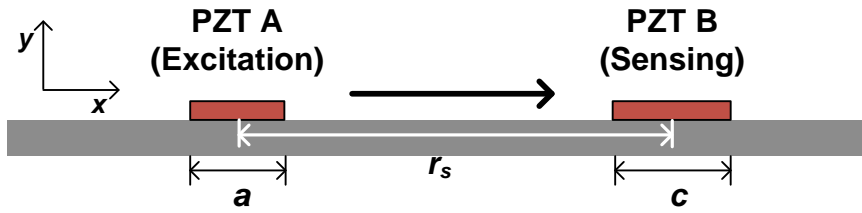
$$V_{22} = S_{22} \times C_{S_0} + A_{22} \times C_{A_0} = S_{22} \times$$

$$+ A_{22} \times$$

S_{ij} or A_{ij} Scaling factors of the S_0 or A_0 modes in V_{ij}

C_{S_0} or C_{A_0} : A common function of S_0 or A_0 modes in V_{ij}

Relationship between Actuator/Sensor Size and Response at a Sensor PZT



$$u_x \propto \sin(\xi a) \quad (\text{Ref 1})$$

$$V(t) \propto \frac{\sin(\xi a) \sin(\xi c)}{c} \quad (\text{Ref 2})$$

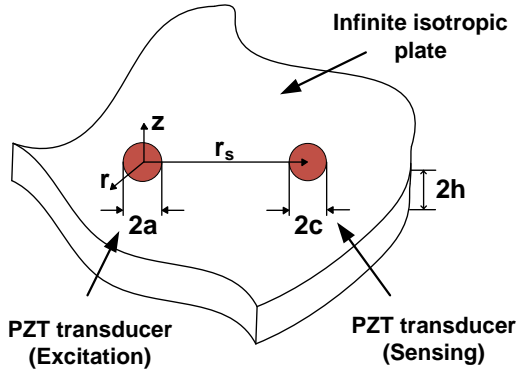
$$u_r(t) \propto a J_1(\xi a) \quad (\text{Ref 3})$$

$$V(t) \propto a J_1(\xi a) \times ? \quad (\text{Ref 4})$$

• ξ Is wavenumber.

1. V. Giurgiutiu., "Lamb wave generation with piezoelectric wafer active sensors for structural health monitoring," SPIE. 5056, 111-122 (2003)
2. A. Raghavan et al, "Modeling of piezoelectric-based Lamb-wave generation and sensing for structural health monitoring," SPIE. 5391 (2004)
3. Ajay Raghavan et al, "Finite-dimensional piezoelectric transducer modeling for guided wave based structural health monitoring," *Smart Mater. Struct.*, 14, pp. 1448-1461 (2005)
4. H. Sohn et al, "Lamb wave tuning curve calibration for surface-bonded piezoelectric transducers," *Smart Mater. Struct.* 19, 015007 (2010)

Three Noticeable Factors of Theoretical Equations for 3D a Circular PZT Actuator and Circular PZT Sensor



$$V(t) = -i \frac{2\tau_0 E_s h_s g_{31} a}{\mu c} \sqrt{\frac{2\pi}{r_s}} \left[\frac{1}{\sqrt{\xi^{S_0}}} J_1(\xi^{S_0} a) J_1(\xi^{S_0} c) \frac{N_s(\xi^{S_0})}{D_s'(\xi^{S_0})} e^{i(\omega t - \frac{\pi}{4} + \xi^{S_0} r_s)} + \frac{1}{\sqrt{\xi^{A_0}}} J_1(\xi^{A_0} a) J_1(\xi^{A_0} c) \frac{N_s(\xi^{A_0})}{D_s'(\xi^{A_0})} e^{i(\omega t - \frac{\pi}{4} + \xi^{A_0} r_s)} \right]$$

$$V(t) \propto a J_1(\xi a) \times \frac{J_1(\xi c)}{c}$$

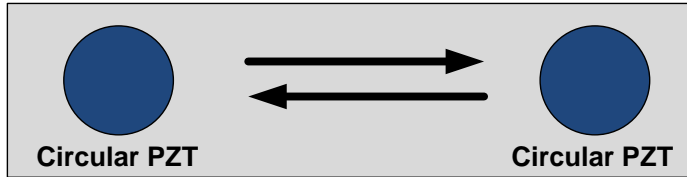
'Maclaurin series', 'asymptotic Hankel function' and 'poisson integral of the Bessel function' are used for the derivation of the analytical solution of the Lamb wave response at a circular PZT

- The amplitudes of the S_0 and A_0 modes are functions of **the excitation and sensing PZT sizes (a and c)**
- In the fixed distance between the sensing and excitation PZTs, **signal phases** does not change with respect to the variations of the PZT size
- There is no coupled term between the excitation/sensing PZT sizes (a and c) and distance (r_s)

Formulation of the Decomposition Technique



Circular PZT actuator & circular PZT sensor



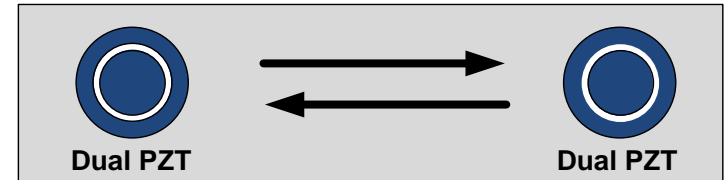
$$V(t) = C^{S_0}(r_s) S^{S_0}(a, c) + C^{A_0}(r_s) S^{A_0}(a, c)$$

where $C^{S_0}(r_s) = -i \frac{2\sqrt{2\pi\tau_0} E_s h_s g_{31}}{\mu \sqrt{\xi^{S_0} r_s}} \frac{N_S(\xi^{S_0})}{D_S'(\xi^{S_0})} e^{i(\omega t - \frac{\pi}{4} + \xi^{S_0} r_s)}$

$$S^{S_0}(a, c) = \frac{a}{c} J_1(\xi^{S_0} a) J_1(\xi^{S_0} c)$$

$C^{A_0}(r_s)$ and $S^{A_0}(a, c)$ are defined in a similar fashion.

Dual PZT actuator & dual PZT sensor



$$\mathbf{V} = \mathbf{S}\mathbf{C}$$

$$\mathbf{V} = \begin{bmatrix} V_{11} \\ V_{12} \\ \vdots \\ V_{33} \end{bmatrix}, \mathbf{S} = \begin{bmatrix} S_{11} & A_{11} \\ S_{12} & A_{12} \\ \vdots & \vdots \\ S_{33} & A_{33} \end{bmatrix}, \mathbf{C} = \begin{bmatrix} C^{S_0}(r_s) \\ C^{A_0}(r_s) \end{bmatrix}$$

V_{ij} : Nine different signals measured from dual PZTs

S_{ij} and A_{ij} : Scaling factors for the S_0 and A_0 mode

Detail Procedure of the Proposed Mode Decomposition Technique



1. A total of nine V_{ij} are obtained by activating different parts (the outer ring, inner circle or both) of the excitation and sensing dual PZTs
2. For the given sizes of the dual PZTs, the corresponding scaling factors (S_{ij} and A_{ij}) can be analytically or experimentally computed.
3. The matrix \mathbf{C} can be estimated by taking the pseudo-inverse of the scaling factor matrix \mathbf{S} and pre-multiply it to the matrix \mathbf{V} .

$$\mathbf{V} = \mathbf{S}\mathbf{C} \quad \longrightarrow \quad \mathbf{S}^\dagger \mathbf{V} = \mathbf{C} \quad \text{'\dagger' is the pseudo-inverse}$$

4. Finally, either the S_0 or A_0 mode in any measured signal can be decomposed and isolated.

Ex) The contribution of the S_0 mode in V_{13} can be obtained as $S_{13} \times C^{S_0}(r_s)$.

The contribution of the A_0 mode in V_{13} can be obtained as $A_{13} \times C^{A_0}(r_s)$.

Estimation of the Scaling Factors



What is the practical problem?

- The effective PZT size becomes less than the physical PZT size due to bonding layer
- Material properties of the structure continuously vary due to temperature

Estimation of the scaling factors from measured signals

$$\begin{bmatrix} V_{11} \\ V_{12} \\ \vdots \\ V_{33} \end{bmatrix} = \begin{bmatrix} S_{11} & A_{11} \\ S_{12} & A_{12} \\ \vdots & \vdots \\ S_{33} & A_{33} \end{bmatrix} \begin{bmatrix} C^{S_0}(r_s) \\ C^{A_0}(r_s) \end{bmatrix} \quad \longrightarrow \quad \begin{bmatrix} V_{11} \\ V_{12} \\ \vdots \\ V_{33} \end{bmatrix} = \begin{bmatrix} \tilde{S}_{11} & \tilde{A}_{11} \\ \tilde{S}_{12} & \tilde{A}_{12} \\ \vdots & \vdots \\ \tilde{S}_{33} & \tilde{A}_{33} \end{bmatrix} \begin{bmatrix} S_{11} C^{S_0} \\ A_{11} C^{A_0} \end{bmatrix} \quad \text{where } \tilde{S}_{ij} = S_{ij} / S_{11}$$

$$\tilde{A}_{ij} = A_{ij} / A_{11}$$

$$\tilde{S}_{ij} = S_{ij} / S_{11} = \frac{(S_{ij} \times C^{S_0}(r_s))}{(S_{11} \times C^{S_0}(r_s))}$$

Amplitude of the S_0 mode in V_{ij}

Amplitude of the S_0 mode in V_{11}

$\tilde{S}_{ij}(\tilde{A}_{ij})$ is the normalized scaling factor



Requirement

The first arriving S_0 and A_0 modes are well separated in the time domain so that their amplitude can be easily estimated.

Problem

When the distance between the excitation and sensing PZTs is too short or there are multiple reflection paths, the estimation of the amplitudes of the first arriving S_0 and A_0 modes can be challenging.

Solution

A pair of excitation and sensing PZTs is placed with a longer spacing so that the first arrivals of the S_0 and A_0 modes can be well separated.

The normalized scaling factors estimated from a single long path can be used for the mode decomposition in all the other paths with varying path lengths as long as they use the same sizes of the dual PZTs.



1 Introduction

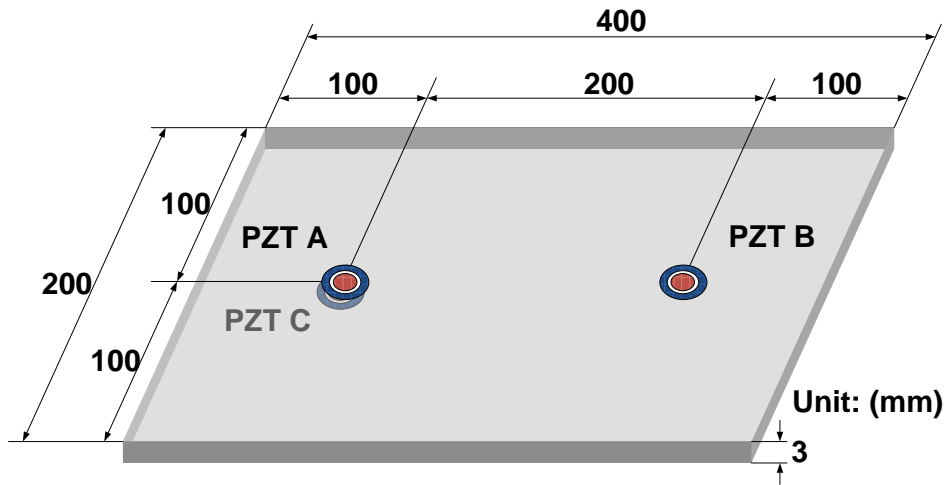
2 Theoretical Formulation

3 Numerical Simulation

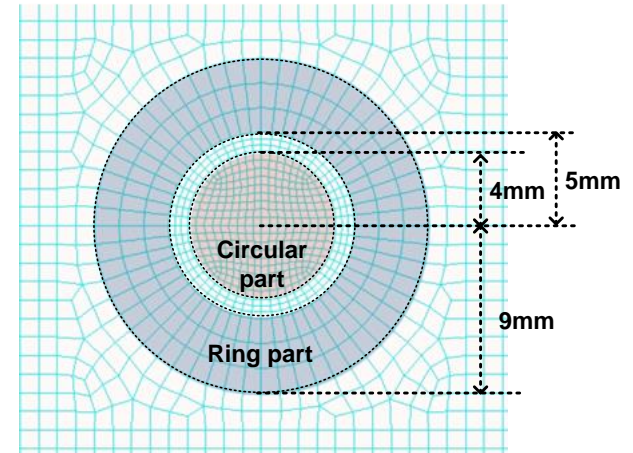
4 Test Results

5 Conclusion

3D Numerical Simulation



Configuration of simulated plate



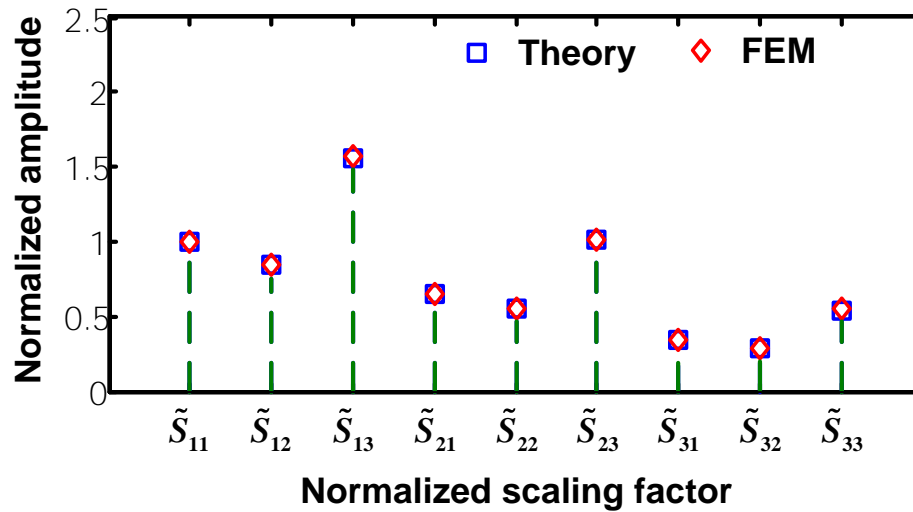
Dimension of the dual PZT

Input	Pin-force, 180 kHz, 7 cycle toneburst
Material	Aluminum
Sampling rate	5 MHz
Mesh size	1 mm x 1mm x 1mm
Software	MSC/NASTRAN

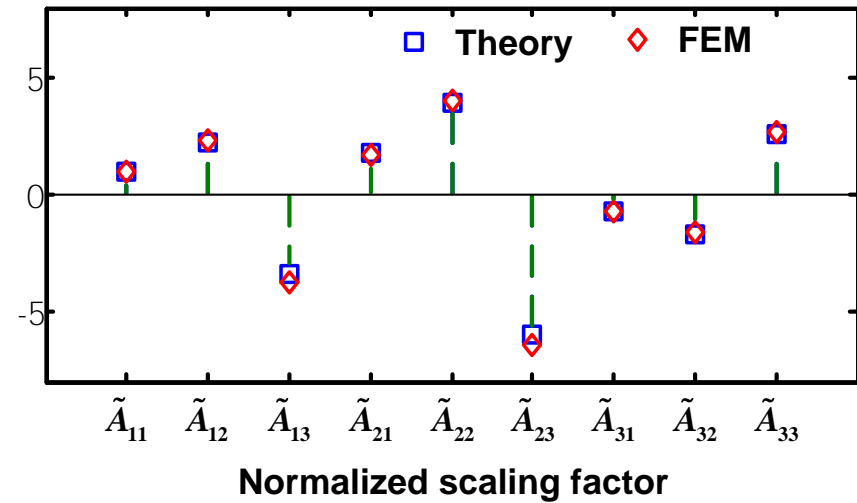
Comparison of the Normalized Scaling Factors Obtained from Numerical Simulation and Theoretical Solution



S_0 mode



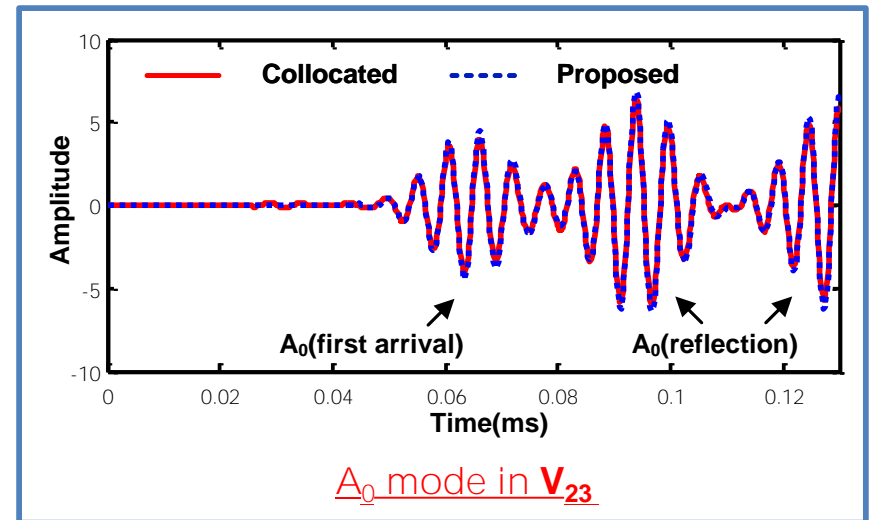
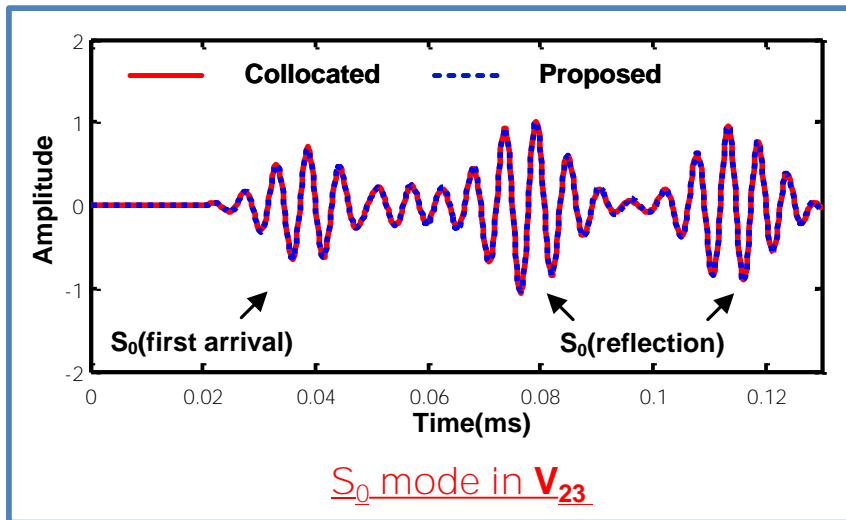
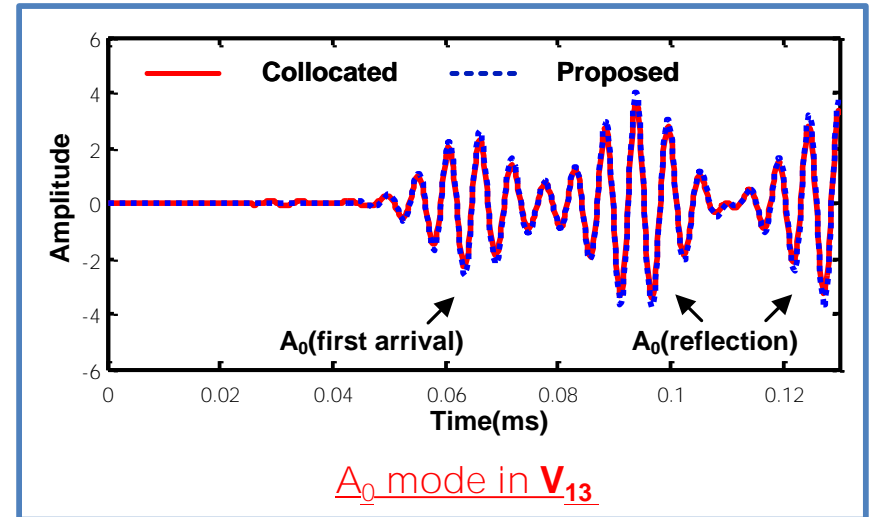
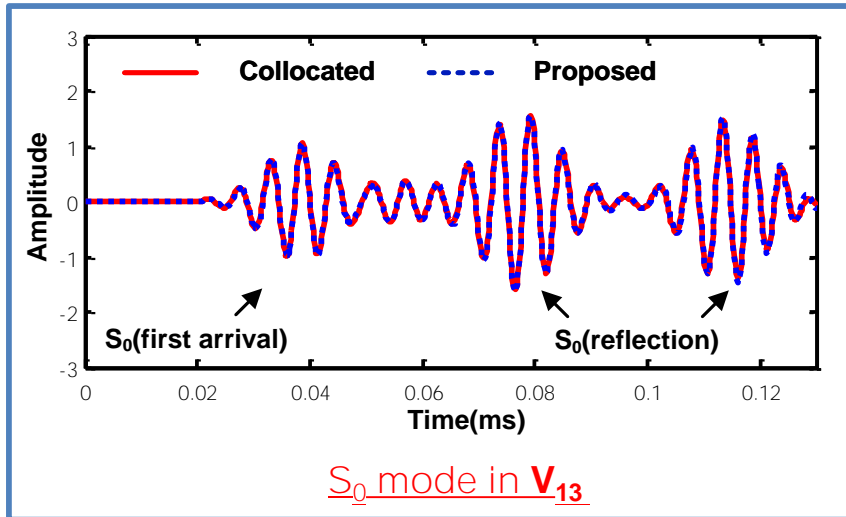
A_0 mode



$$\tilde{S}_{ij} = S_{ij} / S_{11}, \quad \tilde{A}_{ij} = A_{ij} / A_{11}$$

**Numerical and theoretical normalized scaling factors
match well**

Comparison between the S_0 and A_0 Modes Decomposed by the Proposed Technique and the Collocated PZTs





1 Introduction

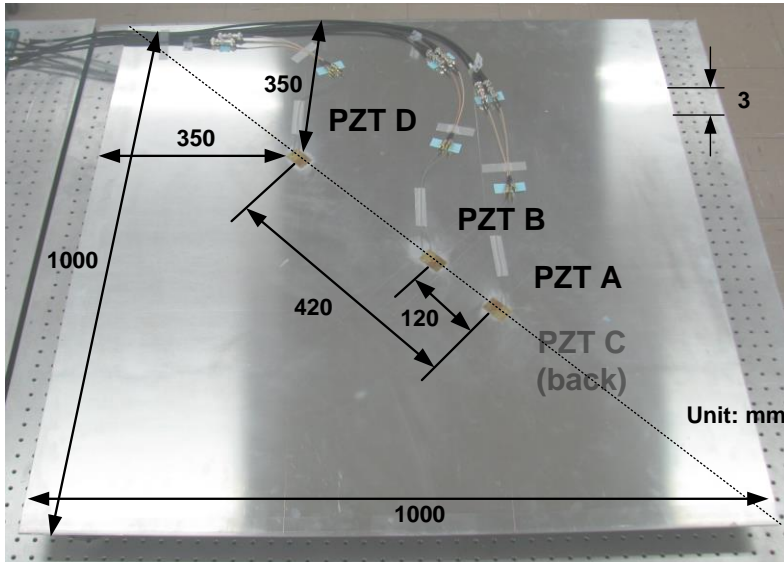
2 Theoretical Formulation

3 Numerical Simulation

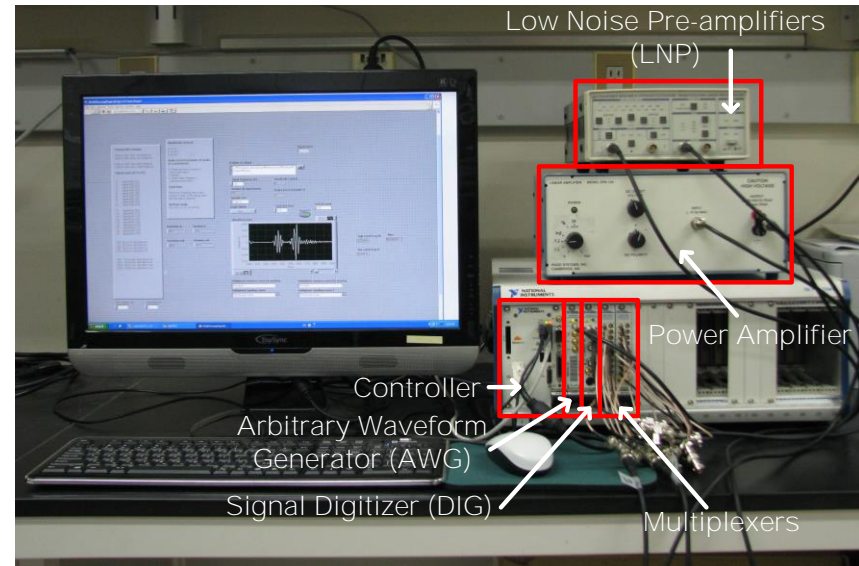
4 Test Results

5 Conclusion

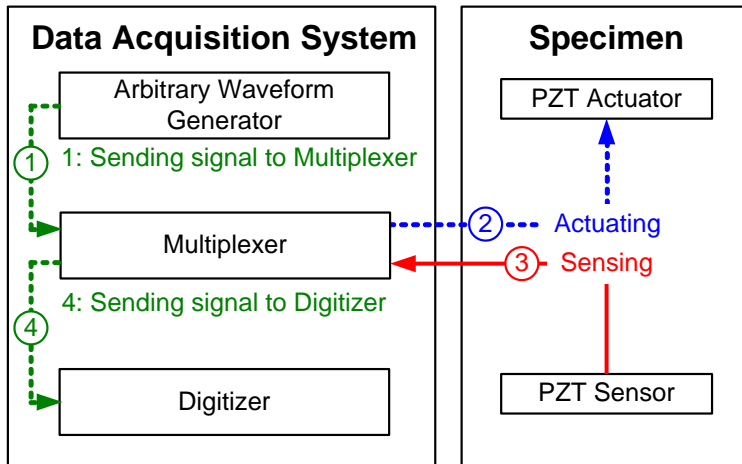
Experimental Setup



Test specimen

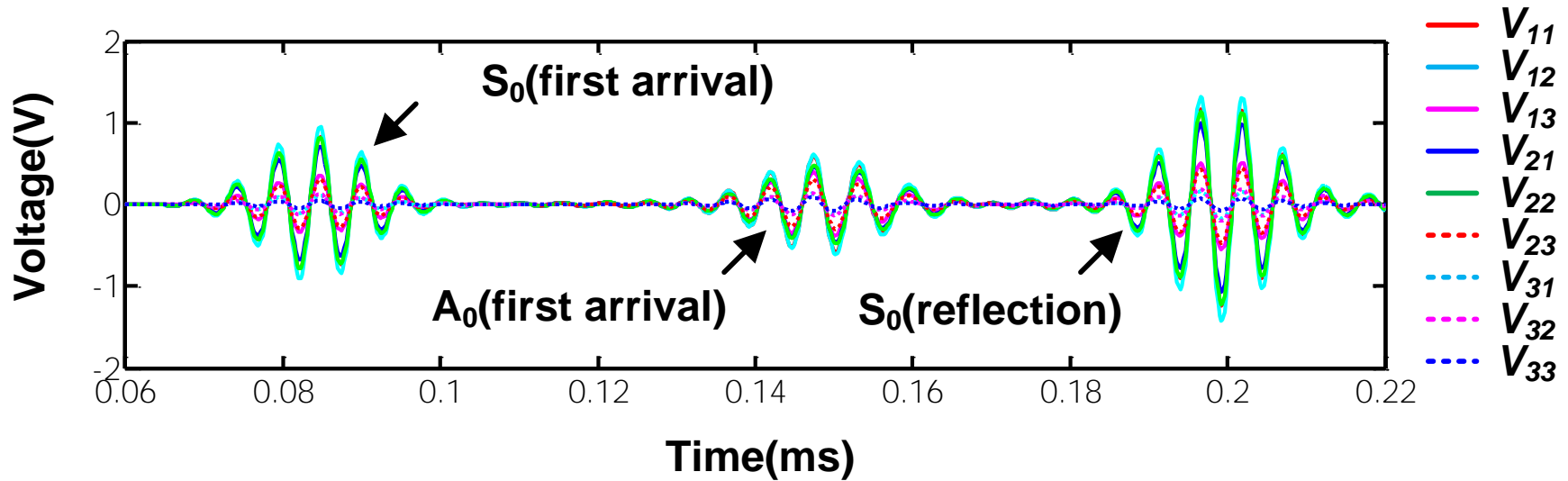


Data acquisition system



- The dimension of each PZT :
 - * 4 packaged dual PZTs
 - * PSI-5A4E type
- Input signal :
 - A 180kHz tone-burst signal with ± 10 peak-to-peak voltage
- Sampling rate : 20MS/s
- Data averaging : 20 times

Comparison of V_{ij} Measured from the Path AD

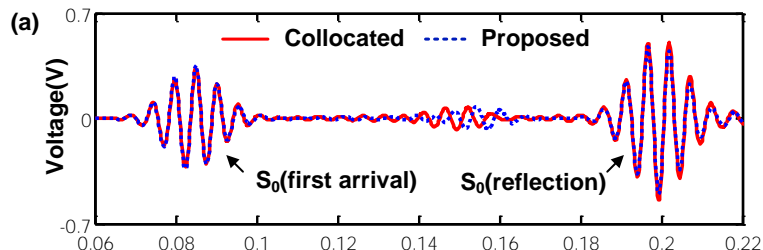


- The amplitudes of the S_0 and A_0 modes are functions of the excitation and sensing PZT sizes
- In the fixed distance between the sensing and excitation PZTs, signal phases does not change with respect to the variations of the PZT size

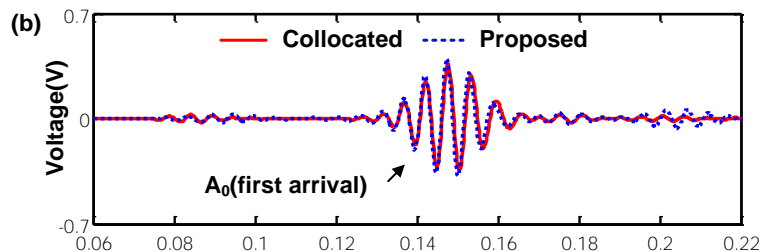
Comparison between the S_0 and A_0 Modes Decomposed by the Proposed Technique and the Collocated PZTs (Path AD)



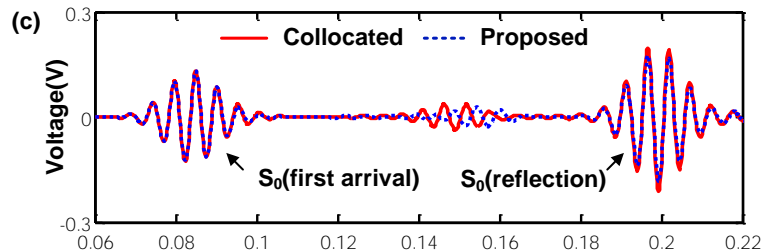
S_0 mode in V_{13}



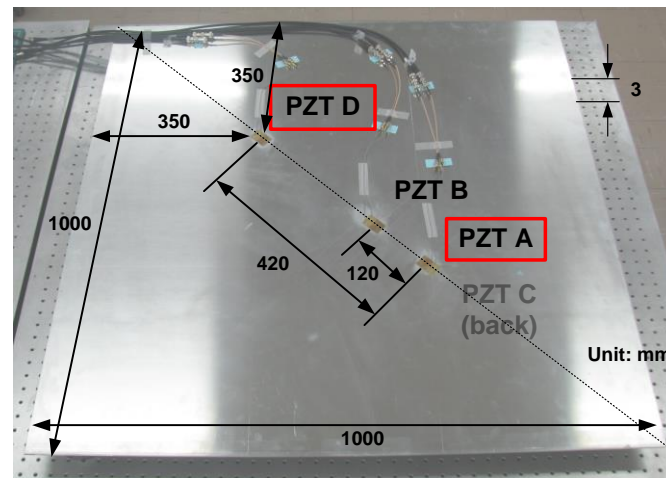
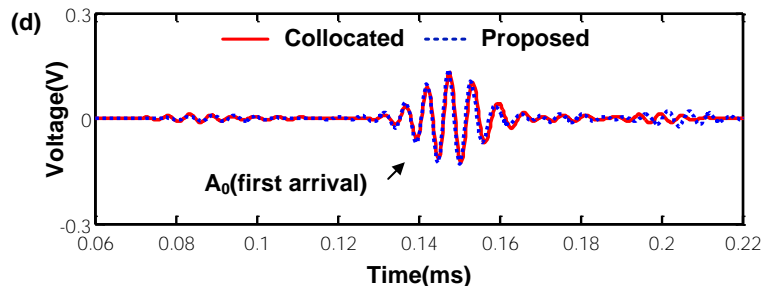
A_0 mode in V_{13}



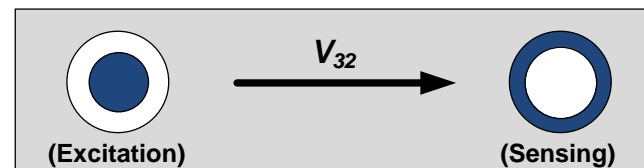
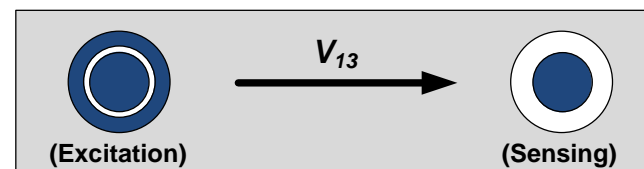
S_0 mode in V_{32}



A_0 mode in V_{32}

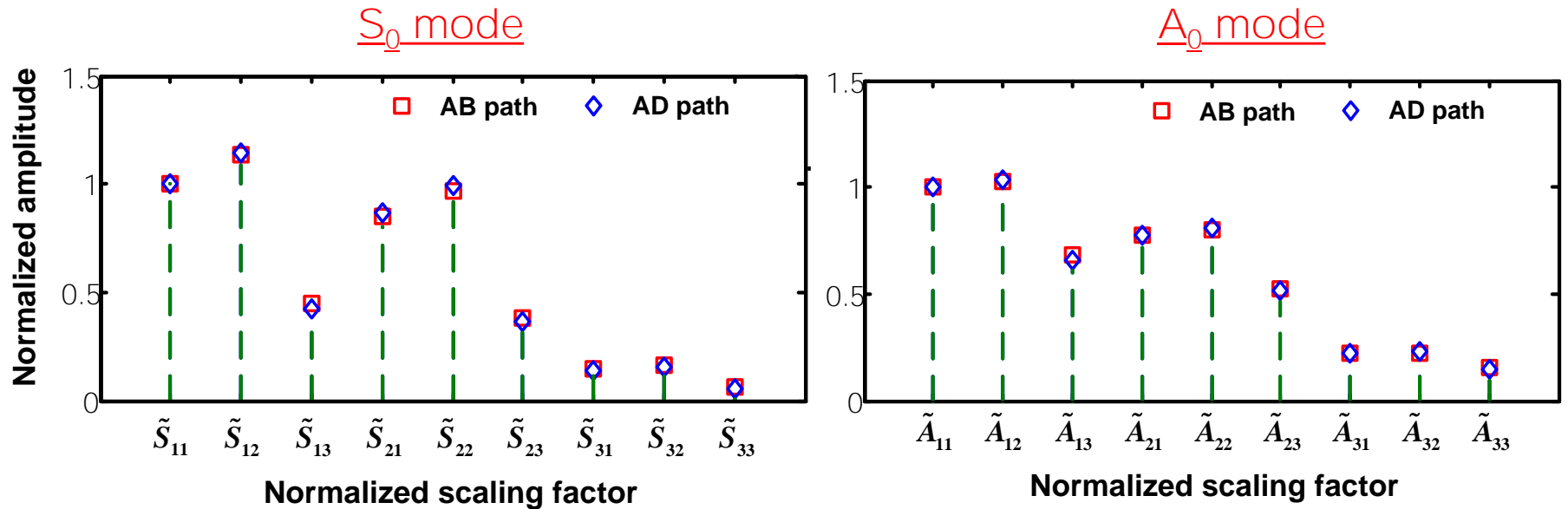


Test specimen



Signal notation

Comparison of the Normalized Scaling Factors of the S_0 and A_0 Modes Obtained from the Paths AB and AD

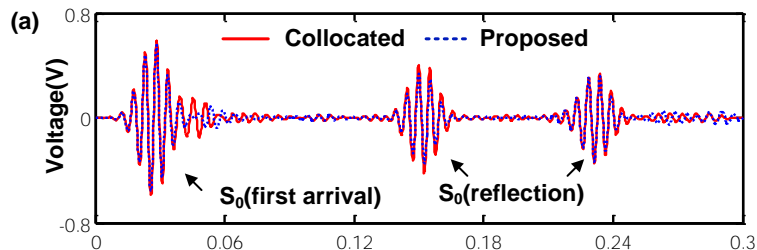


Normalized scaling factors in the path AD were in good agreement with those in the path AB.

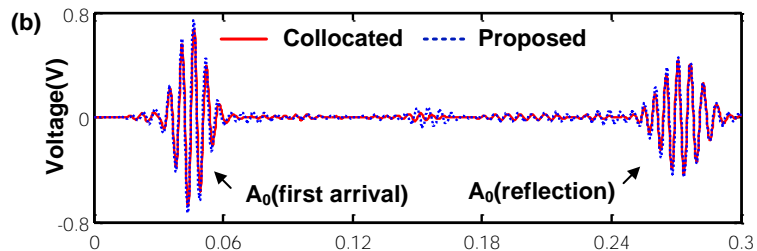
Comparison between the S_0 and A_0 Modes Decomposed by the Proposed Technique and the Collocated PZTs (Path AB)



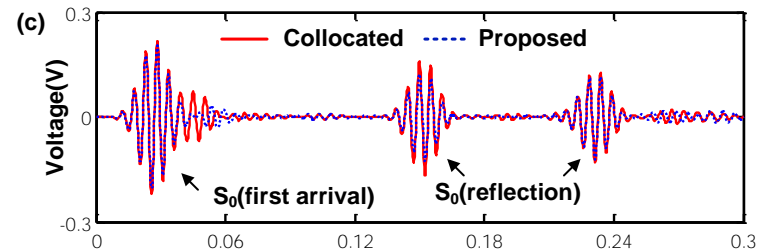
S_0 mode in V_{13}



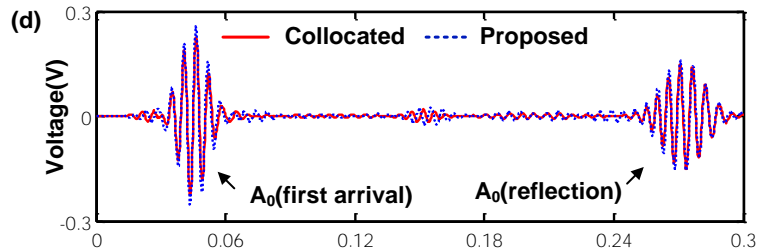
A_0 mode in V_{13}



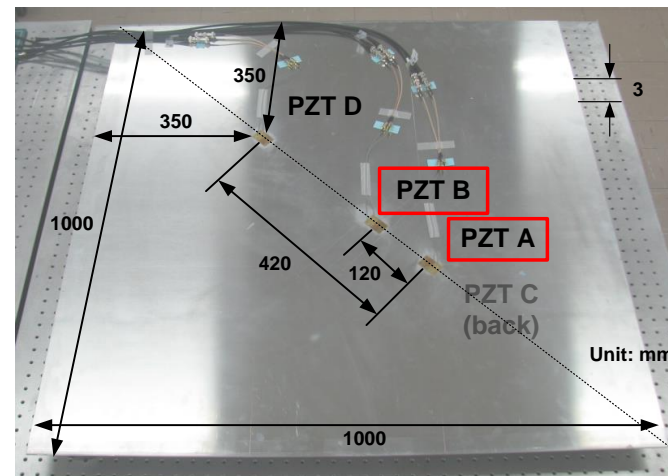
S_0 mode in V_{32}



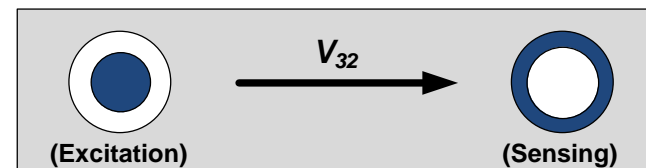
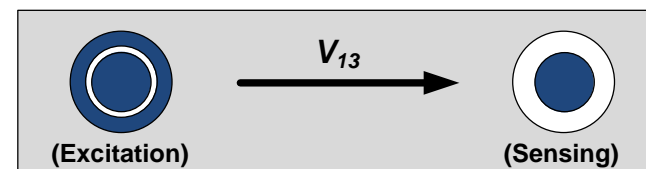
A_0 mode in V_{32}



Time(ms)



Test specimen



Signal notation



1 Introduction

2 Theoretical Formulation

3 Numerical Simulation

4 Test Results

5 Conclusion



Summary

1. Fundamental Lamb wave modes (S_0 and A_0) modes are successfully decomposed by the proposed mode decomposition technique using a pair of dual PZTs
2. The S_0 and A_0 modes can be decomposed at any desired frequency without any other special tuning.

Future study

1. Extend the proposed concept to anisotropic structure and complex geometries with stiffeners or welded joints
2. Effectiveness of the proposed technique on damage detection



- V. Giurgiutiu., "Lamb wave generation with piezoelectric wafer active sensors for structural health monitoring," SPIE. 5056, 111-122 (2003)
- A. Raghavan and C. E. S. Cesnik, "Modeling of piezoelectric-based Lamb-wave generation and sensing for structural health monitoring," SPIE. 5391 (2004)
- H. Sohn, S. J. Lee, "Lamb wave tuning curve calibration for surface-bonded piezoelectric transducers," Smart Mater. Struct. 19, 015007 (2010).
- I. A. Viktorov, Rayleigh and Lamb Waves (Plenum, New York, 1967).
- S. B. Kim, and H. Sohn, "Instantaneous reference-free crack detection based on polarization characteristics of piezoelectric materials," Smart Mater. Struct. 16, 2375-2387 (2007).
- J. L. Rose, S. P. Pelts, and M. J. Quarry, "A comb transducer for mode control in guided wave NDE," IEEE Ultras. Symp. Proc. 857–860 (1996).
- F. L. Degertekin and B. T. Khuri-Yakub, "Single mode lamb wave excitation in thin plates by Hertzian contacts," Appl. Phys. Lett. 69, 146–148 (1996).
- P. D. Wilcox, M. J. S. Lowe, and P. Cawley, "Mode and transducer selection for long range Lamb wave inspection," J. Intell. Mater. Syst. Struct. 12, 553–565 (2001).
- V. Giurgiutiu, "Tuned Lamb wave excitation and detection with piezoelectric wafer active sensors for structural health monitoring," J. Intell. Mater. Syst. Struct. 16, 291–305 (2005).



Do You Have Any Questions ?

I would be happy to help



Backup Slides



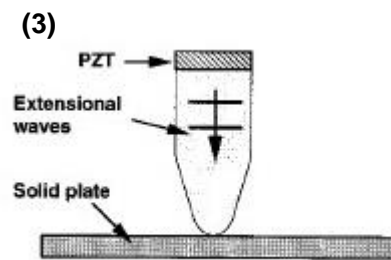
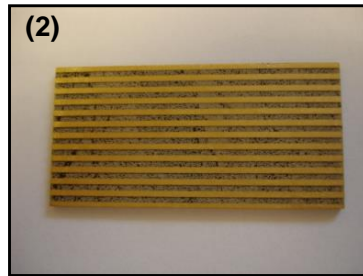
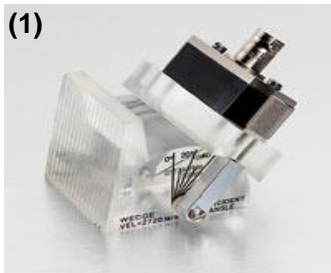
- (1) The target structure has a **uniform thickness** and **isotropic material properties**
- (2) All the dual PZTs installed are **identical** in terms of their sizes and bonding conditions
- (3) The driving frequency range is selected so that only the S_0 and A_0 modes are excited
- (4) Spatial distribution of temperature over the specimen is **uniform** although temperature variation over time is allowed and has no effect on the proposed technique.

Literature Review : Conventional Transducers for Selective Lamb Wave Generation and Sensing



Conventional Techniques

1. Angle wedge tuning using contact and non contact type wedge transducer [Wilcox (2002)]
2. Wavelength-matched linear arrays, using comb transducers [Rose (1998)]
3. Point source point receiver (PS-PR) using Hertzian contacts [Degertekin (1996)]



- (1) Angle wedge transducer
(2) Comb transducer
(3) Hertzian contact transducer

Limitation

1. Too heavy and bulky for online monitoring of structures (ex. airplanes)
2. Directionality for selective Lamb wave mode generation and sensing
3. Not suitable for deployment to large-scale structure due to relatively high cost
4. Manually adjustment of some parameters of the transducer (ex. the incidence angle or the element spacing)



$$\mathbf{V} = \mathbf{S}\mathbf{C}$$

where a_1 , a_2 and a_3 are the outer and the inner radii of the ring PZT and the radius of the inner circular PZT, respectively,

$$\mathbf{V} = \begin{bmatrix} V_{11} \\ V_{12} \\ \vdots \\ V_{33} \end{bmatrix}, \quad \mathbf{S} = \begin{bmatrix} S_{11} & A_{11} \\ S_{12} & A_{12} \\ \vdots & \vdots \\ S_{33} & A_{33} \end{bmatrix}, \quad \mathbf{C} = \begin{bmatrix} C^{S_0}(r_s) \\ C^{A_0}(r_s) \end{bmatrix}$$

$$S_{33} = S^{S_0}(a_3, a_3), \quad S_{23} = S^{S_0}(a_1, a_3) - S^{S_0}(a_2, a_3),$$

$$S_{32} = (K_1 - K_2)^{-1} (K_1 S^{S_0}(a_3, a_1) - K_2 S^{S_0}(a_3, a_2)),$$

$$S_{22} = (K_1 - K_2)^{-1} \begin{bmatrix} K_1 (S^{S_0}(a_1, a_1) - S^{S_0}(a_3, a_1)) \\ -K_2 (S^{S_0}(a_1, a_2) - S^{S_0}(a_3, a_2)) \end{bmatrix},$$

$$S_{21} = (K_1 - K_2 + K_3)^{-1} \{ (K_1 - K_2) S_{22} + K_3 S_{23} \},$$

$$S_{31} = (K_1 - K_2 + K_3)^{-1} \{ (K_1 - K_2) S_{32} + K_3 S_{33} \},$$

$$S_{13} = S_{23} + S_{33}, \quad S_{12} = S_{22} + S_{32}, \quad S_{11} = S_{21} + S_{31},$$

$$K_j = \pi(a_j)^2,$$

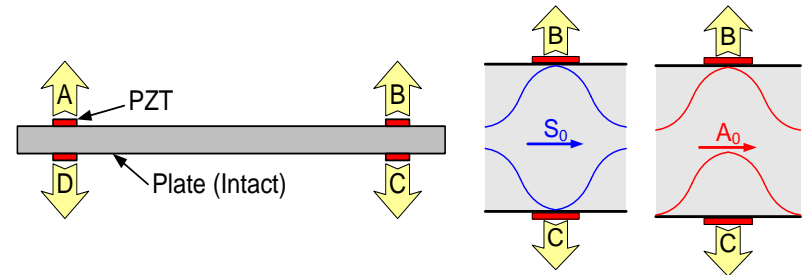
A_{ij} are defined in a similar fashion using $S^{A_0}(a_i, a_j)$ and K_j .



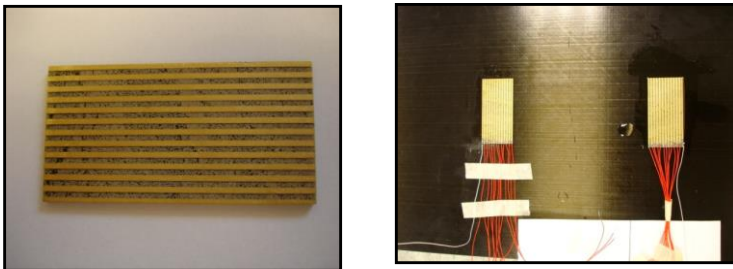
Wedge transducer [Wilcox (2002)]



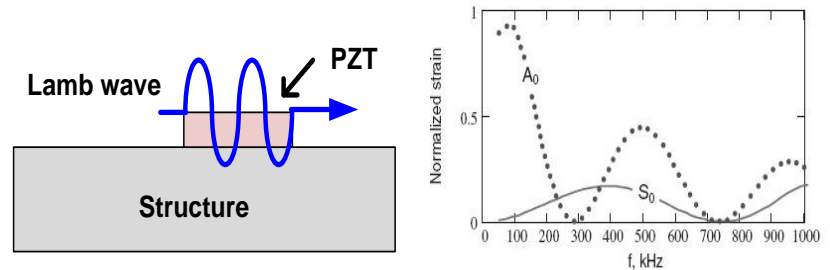
Collocated PZTs on both surfaces [Kim (2007)]



Comb transducer [Rose (1998)]
An array of PZTs with time delays [Gao (2007)]



Tuning of the driving frequency [Giurgitiu (2003)]

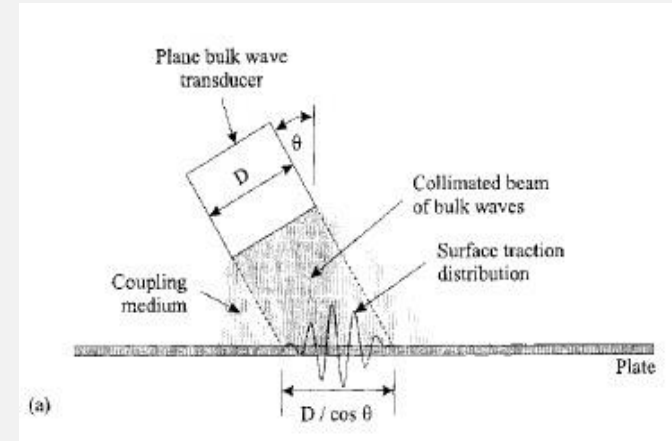


Conventional Techniques for the Lamb Wave Decomposition

- Wedge transducer -



Wedge transducer [Wilcox (2002)]



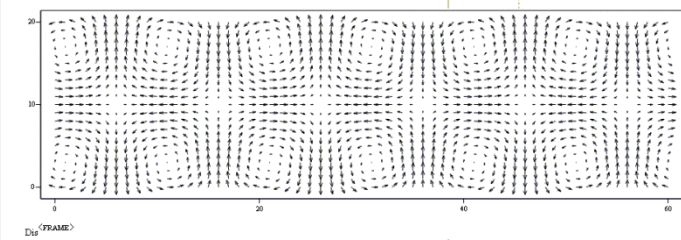
Problems

- Difficulty of setting the angle of incidence with appreciable accuracy
- Consideration of time delay due to block.
- Significant signal attenuation before impinging the inspection material
- Generation of additional reflected waves from interfaces

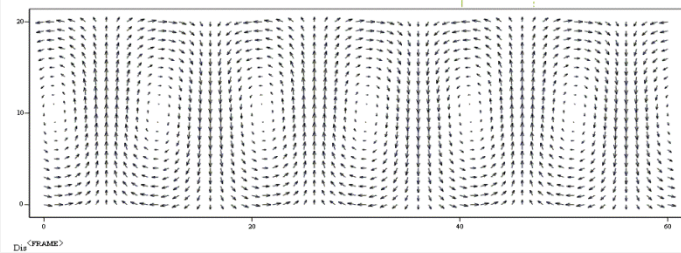
Conventional Techniques for the Lamb Wave Decomposition - Collocated PZTs -



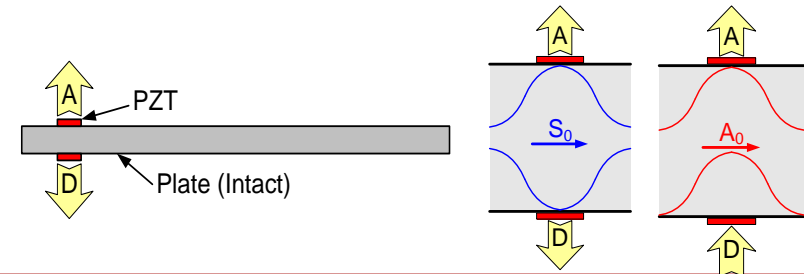
S_0 mode



A_0 mode



Collocated PZTs [Kim and Sohn (2007)]



Problems



Conventional Techniques for the Lamb Wave Decomposition

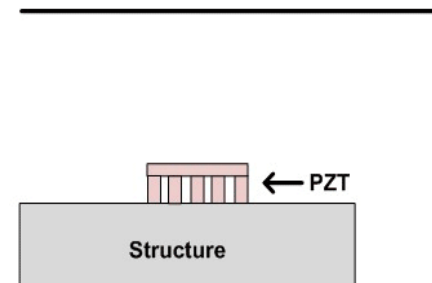
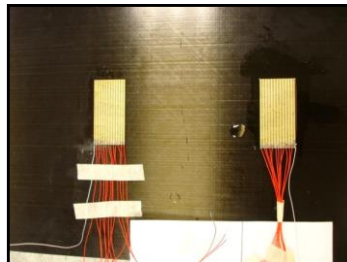
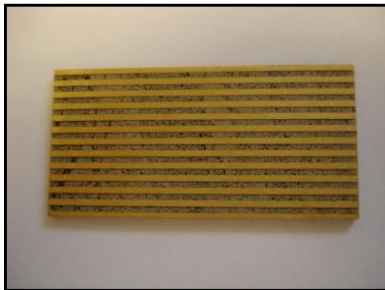
- Comb transducer -



Problems

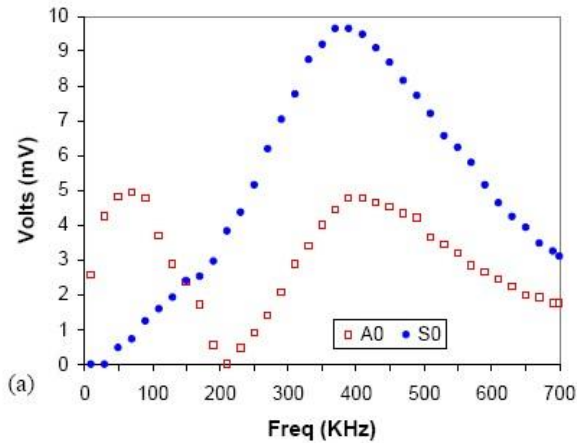
- Decomposition of Lamb waves at a specific frequency
- Needs for a multi channel data acquisition system
- Sensitive to prescribed time delay profiles or wavelength

Comb transducer [Rose (1998)]
An array of PZTs with time delays [Gao (2007)]

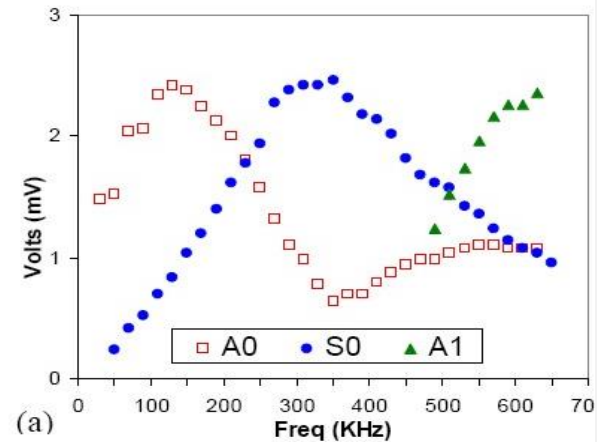


Conventional Techniques for the Lamb Wave Decomposition

- Tuning of the driving frequency -



Aluminum 2024-T3 1.07 mm

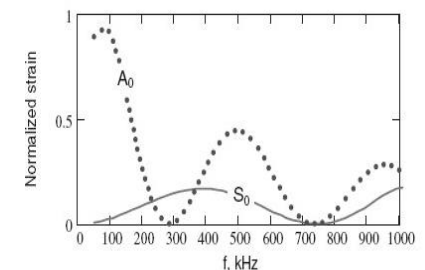
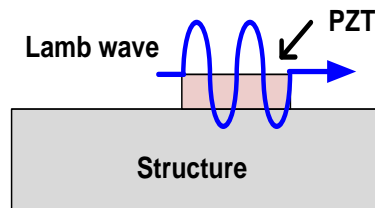


Aluminum 2024-T3 7 mm

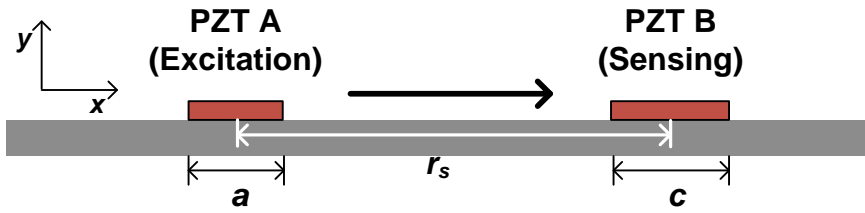
Problems

- Decomposition of Lamb waves at a specific frequency
- Needs for a baseline tuning curve

Tuning of the driving frequency [Giurgitiu (2005)]



Theoretical Response Model for 2D PZTs



$$u_x \propto \sin(\xi a)$$

$$V(t) \propto \frac{\sin(\xi a) \sin(\xi c)}{c}$$

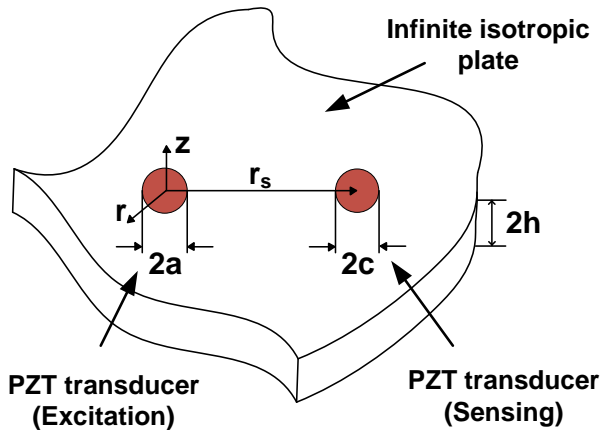
Displacement at x from the PZT A [Giurgiutiu (2003)]

$$u_x(t) = -i \frac{\tau_0}{\mu} \cdot \left[\frac{\sin \xi^{S_0} a}{\xi^{S_0}} \frac{N_S(\xi^{S_0})}{D_S'(\xi^{S_0})} e^{i(\xi^{S_0} x - \omega t)} + \frac{\sin \xi^{A_0} a}{\xi^{A_0}} \frac{N_A(\xi^{A_0})}{D_A'(\xi^{A_0})} e^{i(\xi^{A_0} x - \omega t)} \right]$$

Voltage Response at PZT B [Giurgiutiu (2003)]

$$V(t) = \frac{\tau_0 E_s h_s g_{31}}{\mu} \left[\frac{\sin \xi^{S_0} a \sin \xi^{S_0} c}{\xi^{S_0} 2c} \frac{N_S(\xi^{S_0})}{D_S'(\xi^{S_0})} e^{i(\xi^{S_0} r_s - \omega t)} + \frac{\sin \xi^{A_0} a \sin \xi^{A_0} c}{\xi^{A_0} 2c} \frac{N_S(\xi^{A_0})}{D_S'(\xi^{A_0})} e^{i(\xi^{A_0} r_s - \omega t)} \right]$$

Theoretical Response Model for 3D Circular PZTs



$$u_r(t) \propto aJ_1(\xi a)$$

$$V(t) \propto aJ_1(\xi a) \times ?$$

Displacement at x from the PZT A [Ajay(2004)]

$$u_r(r, z = b) = -\pi i \frac{\tau_0 a}{\mu} e^{i\omega t} \cdot \left[J_1(\xi^{S_0} a) \frac{N_S(\xi^{S_0})}{D_S'(\xi^{S_0})} H_1^{(2)}(\xi^{S_0} r) + J_1(\xi^{A_0} a) \frac{N_A(\xi^{A_0})}{D_A'(\xi^{A_0})} H_1^{(2)}(\xi^{A_0} r) \right]$$

Voltage Response at PZT B [Lee and Sohn (2010)]

$$V(t) = -i \frac{\tau_0 E_s h_s g_{31} a}{\mu c^2} e^{i\omega t} \cdot J_1(\xi^{S_0} a) \frac{N_S(\xi^{S_0})}{D_S'(\xi^{S_0})} \int_{r_s-c}^{r_s+c} \left\{ \xi^{S_0} r H_0^{(2)}(\xi^{S_0} r) \cdot 2 \tan^{-1} \left(\sqrt{\frac{4r^2 r_s^2}{(r^2 + r_s^2 - c^2)^2} - 1} \right) \right\} dr$$

Existing Theoretical Models for PZT Responses



A 2D rectangular PZT sensor's interaction
with Lamb waves (Ref.1)



A 3D circular PZT actuator & a rectangular
PZT sensor (Ref.2)



A 3D rectangular PZT actuator & a
Rectangular PZT sensor (Ref.3)



A 3D circular PZT actuator & a circular
PZT sensor (Ref.4)